Accurate Biot-Savart Routines with Correct Asymptotic Behavior

Jonathan Schilling[a,*], Jakob Svensson[a], Joachim Geiger[a]

[a] *Max-Planck-Institute for Plasma Physics, Wendelsteinstrasse 1, 17489 Greifswald, Germany*

Abstract

A set of routines to compute the magnetic vector potential and magnetic field of two types of current carriers is presented. The (infinitely thin) current carrier types are a straight wire segment and a circular wire loop. The routines are highly accurate and exhibit the correct asymptotic behavior far away from and close to the current carrier. A suitable global set of test points is introduced and the methods presented in this work are tested against results obtained using arbitrary-precision arithmetic on all test points. The results are accurate to approximately 16 decimal digits of precision when computed using 64 bit floating point arithmetic, with few exceptions where accuracy drops to 12 digits. These primitive types can be used to make up more complex current carrier arrangements, such as a current along a polygon (by means of defining straight wire segments from point to point of the polygon) and a multi-winding coil with circular cross-section (by positioning circular wire loops at appropriate positions in the coils cross-section). Reference data is provided along with the code to compute it for testing the reader's routines against this work.

Keywords: magnetostatics; Biot-Savart; straight wire segment; circular wire loop; magnetic vector potential; magnetic field

---

PROGRAM SUMMARY

Program Title: abscab: Accurate Biot-Savart routines with Correct Asymptotic Behavior

*Corresponding author.
E-mail address: jonathan.schilling@ipp.mpg.de

CPC Library link to program files: (to be added by Technical Editor)
Developer's repository link: https://github.com/jonathanschilling/abscab
Code Ocean capsule: (to be added by Technical Editor)
Licensing provisions(please choose one): Apache-2.0
Programming language: C
Supplementary material:
Nature of problem(approx. 50-250 words):
Solution method(approx. 50-250 words):
Additional comments including restrictions and unusual features (approx. 50-250 words):

References

[1] Reference 1

[2] Reference 2

[3] Reference 3

1. Introduction

Usually, the magnetic field is denoted by $\mathbf{H}$ and the magnetic flux density $\mathbf{B}$ is then given by $\mathbf{B} = \mu_0 \mu_\mathrm{r} \mathbf{H}$, where μ_0 is the vacuum magnetic permeability and μ_r is the relative permeability, taking material properties into account. In the field of plasma physics, these two terms are frequently used synonymously due to the vanishing magnetic susceptibility $|\chi| \ll 1$ of the plasma, leading to $\mu_r = 1 + \chi \approx 1$. Then, magnetic field and magnetic flux density only differ by the scaling factor μ_0.

2. Methods

In this section, the methods used to compute the magnetic vector potential and the magnetic field of a straight wire segment and a circular wire loop are established.

2.1. Straight Wire Segment

The straight wire segment is handled first. The basic geometry of a single wire segment is shown in Fig. 1.

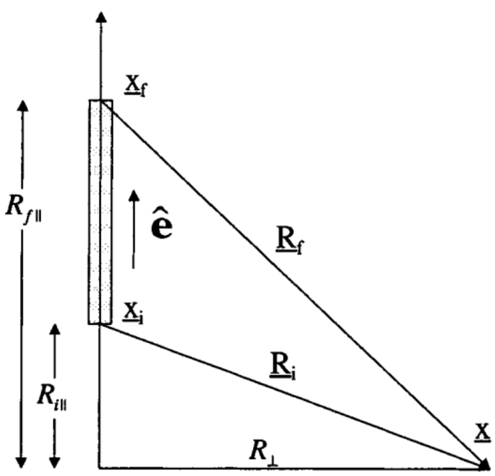

Figure 1: Geometry of a single wire segment. After Fig. 1 in Ref. [1].

2.1.1. Magnetic Vector Potential

The magnetic vector potential of a straight wire segment only has component A_z parallel to the wire that is given by:

$$A_z(\rho, z) = \frac{\mu_0 I}{4\pi} \ln\left(\frac{1+\epsilon}{1-\epsilon}\right) \tag{1}$$

with

$$\epsilon = \frac{L}{R_i + R_f} \tag{2}$$

$$R_i = \sqrt{\rho^2 + z^2} \tag{3}$$

$$R_f = \sqrt{\rho^2 + (1-z)^2}\,. \tag{4}$$

Here, we use normalized coordinates $\rho' = \rho/L$ and $z' = z/L$. This leads to the following expressions for $r_i = R_i/L$ and $r_f = R_f/L$:

$$r_i = \sqrt{\rho'^2 + z'^2} \tag{5}$$

$$r_f = \sqrt{\rho'^2 + (1 - z')^2} \tag{6}$$

$$\epsilon = \frac{1}{r_i + r_f} \,. \tag{7}$$

A common prefactor depending on the current I and μ_0 is split off:

$$A_z(\rho, z) = \frac{\mu_0 I}{2\pi} \tilde{A}_z(\rho', z') \tag{8}$$

with

$$\tilde{A}_z(\rho', z') = \frac{1}{2} \ln\left(\frac{1+\epsilon}{1-\epsilon}\right) = \operatorname{atanh}(\epsilon) \,. \tag{9}$$

The rest of this section can thus focus on accurate computation of $\tilde{A}_z(\rho', z')$.

The region close to the wire segment ("near-field") is handled by one of the following three formulations. The parameter ϵ approaches a value of 1 as the location of the evaluation point comes closer to the wire segment. Thus, the denominator in Eqn. (9) vanishes, leading to a logarithmic singularity in $\tilde{A}_z$ as the evaluation point (ρ', z') gets nearer to the wire segment. It is therefore favorable to formulate the near-field method in terms of $(1 - \epsilon)$:

$$1 - \epsilon = 1 - \frac{1}{r_i + r_f} = \frac{r_i + r_f - 1}{r_i + r_f} = \frac{r_i + r_f - 1}{(r_i + r_f - 1) + 1} = \frac{n}{n+1} \tag{10}$$

with $n \equiv r_i + r_f - 1$ approaching 0 as the evaluation point approaches the wire segment. Inserting this formulation for $1 - \epsilon$ into Eqn. (9) leads to:

$$\begin{aligned}
\tilde{A}_{z,\mathrm{nf}}(\rho', z') &= \frac{1}{2}\left[\ln\left(2 - (1-\epsilon)\right) - \ln\left(1-\epsilon\right)\right] \\
&= \frac{1}{2}\left[\ln\left(2 - \frac{n}{n+1}\right) - \ln\left(\frac{n}{n+1}\right)\right] \\
&= \frac{1}{2}\left[\ln\left(\frac{2(n+1) - n}{n+1}\right) - \ln\left(\frac{n}{n+1}\right)\right] \\
&= \frac{1}{2}\left[\ln\left(n+2\right) \cancel{- \ln\left(n+1\right)} - \ln\left(n\right) \cancel{+ \ln\left(n+1\right)}\right] \\
&= \frac{1}{2}\left[\ln\left(n+2\right) - \ln\left(n\right)\right] \,.
\end{aligned} \tag{11}$$

The subscript "nf" was introduced to indicate that this formulation shall only be used for the near-field. The method used to compute n still has to be switched depending to the exact location of the evaluation point:

$$n = \begin{cases} n_{6a} & : z' \geq 1 \text{ or } \rho'/(1-z') \geq 1 \\ n_{6b} & : z' \geq 0 \text{ and } \rho'/z' \leq 1 \\ n_{6c} & : \text{else} \end{cases} . \tag{12}$$

The first special case introduces a nutritious zero $(-z' + z')$ into n:

$$n_{6a} = (r_i - z') + r_f + (z' - 1) . \tag{13}$$

The first contribution to n is then computed as follows:

$$r_i - z' = 2z' \sin^2(\alpha/2)/\cos(\alpha) \tag{14}$$

with $\alpha = \texttt{atan2}(\rho', z')$. Additionally, r_f is computed via Eqn. (6) and $(z'-1)$ is computed directly. The second special case is based on the first one and introduces another angle β used to compute $r_f + (z' - 1)$ directly:

$$(r_f + z' - 1) = 2(1 - z') \sin^2(\beta/2)/\cos(\beta) \tag{15}$$

with $\beta = \texttt{atan2}(\rho', 1 - z')$. Then, n is computed as:

$$n_{6b} = (r_i - z') + (r_f + z' - 1) \tag{16}$$

with $(r_i - z')$ from Eqn. (14) and $(r_f + z' - 1)$ from Eqn. (15). The third special case is formulated slightly differently. Here, $(r_f - 1)$ is formulated as:

$$r_f - 1 = 2r_f \sin^2(\beta/2) - z' \tag{17}$$

with β as in the second special case and r_i and r_f from Eqn. (5) and Eqn. (6), respectively. This leads to:

$$n_{6c} = r_i + (r_f - 1) \tag{18}$$

with $(r_f - 1)$ from Eqn. (17). This concludes the methods for the near-field evaluation. Two further special cases are considered next: $\rho' = 0$ and the combined case $(z' = 0,\ z' = 1)$. For the case of $\rho' = 0$, the following formulation should be used:

$$\tilde{A}_z(\rho' = 0, z') = \begin{cases} \tilde{A}_2(z') & : z' < 1 \text{ or } z' > 2 \\ \tilde{A}_2 b(z') & : \text{else, except } z' \in [0, 1] \end{cases} \tag{19}$$

with

$$\tilde{A}_2(z') = \operatorname{atanh}\left(\frac{1}{|z'| + |1 - z'|}\right) \tag{20}$$

and

$$\tilde{A}_2 b(z') = \frac{1}{2}\operatorname{sgn}(z') \ln\left(\left|\frac{z'}{1 - z'}\right|\right) . \tag{21}$$

The following formulation should be used for the cases $z' = 0$ or $z' = 1$:

$$\tilde{A}_z(\rho', z' \in \{0, 1\}) = \begin{cases} \tilde{A}_3(\rho') & : \rho' > 1 \\ \tilde{A}_b b(\rho') & : \text{else} \end{cases} \tag{22}$$

with

$$\tilde{A}_3(z') = \operatorname{atanh}\left(\frac{1}{\rho' + \sqrt{\rho'^2 + 1}}\right) \tag{23}$$

and

$$\tilde{A}_3 b(z') = \frac{1}{2} \ln\left(\frac{\rho' c + 1 + c}{\rho' c + 2s^2}\right) \tag{24}$$

$$c = \cos(\alpha) = \left[\rho'^2 + 1\right]^{-1/2} \tag{25}$$

$$s = \sin(\alpha/2) \tag{26}$$

$$\alpha = \arctan(\rho') . \tag{27}$$

If none of above special cases applies, the following general formulation is used for the "far-field" case:

$$\tilde{A}_{z,\text{ff}}(\rho', z') = \operatorname{atanh}\left(\frac{1}{r_i + r_f}\right) \tag{28}$$

with r_i and r_f from Eqn. (5) and Eqn. (6), respectively. The overall switching between the methods introduced above is done as follows:

$$\tilde{A}_z(\rho', z') = \begin{cases} \tilde{A}_z(\rho' = 0, z') & : \rho' = 0 \\ \tilde{A}_z(\rho', z' \in \{0, 1\}) & : z' \in \{0, 1\} \\ \tilde{A}_{z,\text{nf}}(\rho', z') & : z' \in]-1, 2] \text{ and } \rho' < 1 \\ \tilde{A}_{z,\text{ff}}(\rho', z') & : \text{else} \end{cases} . \tag{29}$$

2.1.2. Magnetic Field

The magnetic field of a straight wire segment only has a tangential component B_φ around the wire that is given by:

$$B_\varphi(\rho, z) = \frac{\mu_0 I}{4\pi} \frac{2L(R_i + R_f)}{R_f} \frac{1}{(R_i + R_f)^2 - L^2} \tag{30}$$

with L, R_i and R_f as in the previous section. Again a normalization factor is split off:

$$B_\varphi(\rho, z) = \frac{\mu_0 I}{4\pi L} \tilde{B}_\varphi(\rho', z') \tag{31}$$

with

$$\begin{aligned} \tilde{B}_\varphi(\rho', z') &= \frac{2L^2(R_i + R_f)}{R_f} \frac{1}{(R_i + R_f)^2 - L^2} \\ &= \left(\frac{r_i}{r_f} + 1 \right) \frac{2}{(r_i + r_f)^2 - 1} \, . \end{aligned} \tag{32}$$

The special case $\rho' = 0$ is handled first:

$$\tilde{B}_\varphi(\rho' = 0, z') = \frac{1}{2} \left(\frac{1}{(1 - z')^2} - \frac{1}{z'(1 - z')} \right) \, . \tag{33}$$

Similarly, a special case for $z' \in \{0, 1\}$ can be derived:

$$\tilde{B}_\varphi(\rho', z' \in \{0, 1\}) = \frac{1}{\rho' \sqrt{\rho'^2 + (1 - z')^2}} \, . \tag{34}$$

The next method handles the evaluation locations far away from the loop as well as a part of the near-field:

$$\tilde{B}_{\varphi,4}(\rho', z') = \left(\frac{r_i}{r_f} + 1 \right) \frac{1}{\rho'^2 + r_i r_f - z'(z' - 1)} \, . \tag{35}$$

For certain evaluation points close to the loop, the terms $r_i r_f$ and $-z'(z' - 1)$ in above formula almost cancel each other. This cancellation introduces a requirement for one more method to compute $\tilde{B}_\varphi(\rho', z')$:

$$\tilde{B}_{\varphi,5}(\rho', z') = \frac{r_i/r_f + 1}{\rho'^2 + z'(1 - z') \frac{2}{\cos(\alpha)} \left(\frac{\sin^2(\beta/2)}{\cos(\beta)} + \sin^2(\alpha/2) \right)} \tag{36}$$

with α and β as introduced for Eqn. (14) and Eqn. (15). The overall switching between the methods introduced above is done as follows:

$$\tilde{B}_\varphi(\rho', z') = \begin{cases} \tilde{B}_\varphi(\rho' = 0, z') & : \ \rho' = 0 \\ \tilde{B}_\varphi(\rho', z' \in \{0, 1\}) & : \ z' \in \{0, 1\} \\ \tilde{B}_{\varphi,4}(\rho', z') & : \ z' \notin]0, 1[\text{ or } \rho' \geq 1 \\ & \quad \text{or } \rho'/(1 - z') \geq 1 \\ & \quad \text{or } \rho'/z' \geq 1 \\ \tilde{B}_{\varphi,5}(\rho', z') & : \ \text{else} \end{cases} . \tag{37}$$

2.2. Circular Wire Loop

The circular wire loop is handled next. The basic geometry of a circular wire loop under consideration here is shown in Fig. 2.

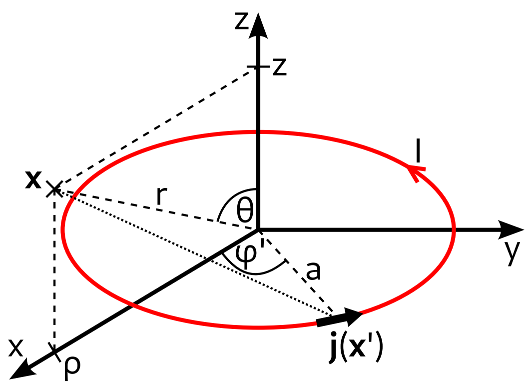

Figure 2: Geometry of a circular wire loop centered at the origin with normal vector aligned with the z-axis. The radius of the loop is denoted a and a current I flows in the indicated direction. The magnetic field and vector potential are to be evaluated at the point $\mathbf{x}$ in the (x, z)-plane.

2.2.1. Magnetic Vector Potential

2.2.2. Magnetic Field

2.3. Transformation to Cartesian Coordinates

Evaluation of the magnetic vector potential A and magnetic field B produced by the current carriers considered in this work happens in cylindrical coordinates ρ and z. It is often more convenient to be able to work in Cartesian coordinates. The methods given in this section show how to transform the evaluation location into cylindrical coordinates in the frame of reference of the current carrier and subsequently transform back the magnetostatic quantities into the global Cartesian coordinate system.

2.3.1. Straight Wire Segment

2.3.2. Circular Wire Loop

Figure 3 illustrates the setup of a circular wire loop.

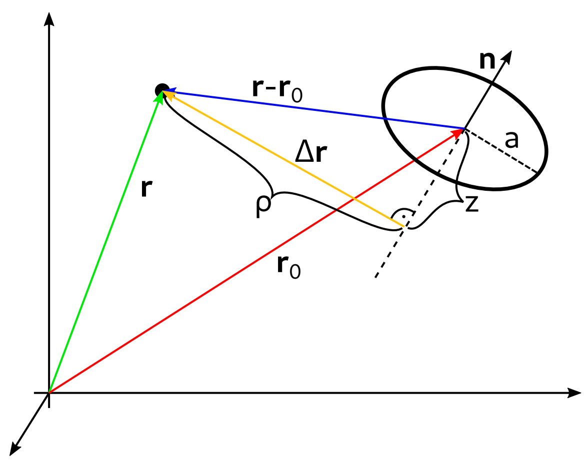

Figure 3: Mapping the components to Cartesian coordinates for an exemplary circular wire loop. The loop is centered around its origin $\mathbf{r}_0$. Its normal vector is denoted $\mathbf{n}$ and defines the orientation of the loop. The radius of the loop is denoted by a. The evaluation location is denoted by $\mathbf{r}$.

The z-axis of the wire loop's coordinate system is defined by the normal vector $\mathbf{n}$:

$$\hat{\mathbf{e}}_z = \frac{\mathbf{n}}{|\mathbf{n}|}\,. \tag{38}$$

The z component of the evaluation location is thus obtained as follows:

$$z = (\mathbf{r} - \mathbf{r}_0) \cdot \hat{\mathbf{e}}_z\,. \tag{39}$$

The normalized z-coordinate z' is then obtained as:

$$z' = \frac{z}{a} = \frac{1}{a}(\mathbf{r} - \mathbf{r}_0) \cdot \hat{\mathbf{e}}_z\,. \tag{40}$$

For the radial coordinate, first the vector $\Delta\mathbf{r}$ is formed:

$$\Delta\mathbf{r} = (\mathbf{r} - \mathbf{r}_0) - z\,\hat{\mathbf{e}}_z \tag{41}$$

and the radial coordinate ρ is then obtained by taking $\rho = |\Delta\mathbf{r}|$. A unit vector in radial direction is formed as follows:

$$\hat{\mathbf{e}}_\rho = \frac{\Delta\mathbf{r}}{\rho}\,. \tag{42}$$

The normalized radial coordinate ρ' is then obtained as:

$$\rho' = \frac{\rho}{a} = \frac{1}{a}|(\mathbf{r} - \mathbf{r}_0) - z\,\hat{\mathbf{e}}_z|\,. \tag{43}$$

The magnetic field of the circular wire loop consists of two cylindrical components, namely B_ρ and B_z. The Cartesian magnetic field components are then computed as follows:

$$\mathbf{B}(\mathbf{r}) = B_\rho\hat{\mathbf{e}}_\rho + B_z\hat{\mathbf{e}}_z\,. \tag{44}$$

The magnetic vector potential only has a component in angular direction in the coordinate system of the wire loop. The corresponding unit vector $\hat{\mathbf{e}}_\varphi$ is then given by $\hat{\mathbf{e}}_\varphi = \hat{\mathbf{e}}_\rho \times \hat{\mathbf{e}}_z$. The vector potential of the circular wire loop in thus in Cartesian coordinates:

$$\mathbf{A}(\mathbf{r}) = A_\varphi\hat{\mathbf{e}}_\varphi\,. \tag{45}$$

2.4. Superposition in multi-filament assemblies

An infinitely thin polygon filament P is described by a list of N points $\mathbf{x}_i$ with $i = 1, ..., N$ in three-dimensional (3D) space and a current I. The $(N-1)$ straight connecting lines between each two consecutive points $\mathbf{x}_i$ and $\mathbf{x}_{i+1}$ are assumed to represent the geometry of a wire which carries the current. If the first and the last point of the polygon filament coincide, the wire forms a closed loop and $\nabla \cdot \mathbf{j} = 0$ is ensured by construction.

The magnetic vector potential $\mathbf{A}(I, \mathbf{x}_i, \mathbf{x}_{i+1}, \mathbf{x})$ and the magnetic field $\mathbf{B}(I, \mathbf{x}_i, \mathbf{x}_{i+1}, \mathbf{x})$ of the wire segments at a location $\mathbf{x}$ can be computed analytically. The resulting contributions from each segment are superposed in order to compute the resulting magnetic field from the full length of the wire:

$$\mathbf{A}(\mathbf{x}) = \sum_{i=1}^{N-1} \mathbf{A}(I, \mathbf{x}_i, \mathbf{x}_{i+1}, \mathbf{x}) \quad \text{and} \tag{46}$$

$$\mathbf{B}(\mathbf{x}) = \sum_{i=1}^{N-1} \mathbf{B}(I, \mathbf{x}_i, \mathbf{x}_{i+1}, \mathbf{x}) \quad . \tag{47}$$

Computationally robust and efficient expressions for $\mathbf{A}(I, \mathbf{x}_i, \mathbf{x}_{i+1}, \mathbf{x})$ and $\mathbf{B}(I, \mathbf{x}_i, \mathbf{x}_{i+1}, \mathbf{x})$ are given in Ref. [1]. The detailed derivation of these expressions is given below.

2.5. Verification Method

The asymptotic behavior of an implementation of above formulas for the magnetic vector potential and magnetic field needs to be tested before using that implementation in daily routine work. A set of critical test points used to check this is shown in Fig. 4 for the case of the circular wire loop.

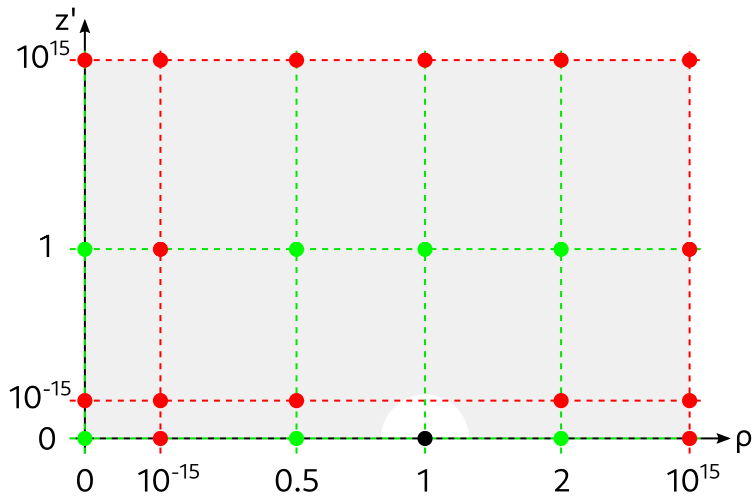

Figure 4: Test points in the R-Z-plane for a circular wire loop (black dot). The axes are labeled in normalized cylindrical coordinates ($\rho' = \rho/a$, $z' = z/a$; a is the radius of the wire loop). Green dashed lines indicate values of ρ' and z' which are well handled by a naive implementation. Green dots denote points at which a naive implementation yields satisfactory results. Red dashed lines indicate values of ρ' and z' which induce the requirement for robust asymptotic behavior. Red dots denote points at which a naive implementation usually fails. The grey shaded area in the background indicates the region in which the reference implementation yields accurate results. Note that the problem is symmetric in z direction, even though only the positive-z quadrant is considered here.

3. Results

4. Discussion

It turns out that most of these problems have been considered in Ref. [4] already.

5. Concluding Remarks

Appendix A. Derivation of General Formulations

The derivations of the starting point formulas presented in Sec. 2 are given here.

Appendix A.1. Straight Wire Segment

The following geometric quantities with $\mathbf{x}_f \equiv \mathbf{x}_{i+1}$ are defined to ease the rest of the derivation:

$$L \equiv |\mathbf{x}_f - \mathbf{x}_i| \quad , \tag{A.1}$$
$$\hat{\mathbf{e}} \equiv (\mathbf{x}_f - \mathbf{x}_i)/L \quad , \tag{A.2}$$
$$\mathbf{R}_i \equiv \mathbf{x} - \mathbf{x}_i \quad , \tag{A.3}$$
$$\mathbf{R}_f \equiv \mathbf{x} - \mathbf{x}_f \quad , \tag{A.4}$$
$$R_i \equiv |\mathbf{R}_i| = |\mathbf{x} - \mathbf{x}_i| \quad , \tag{A.5}$$
$$R_f \equiv |\mathbf{R}_f| = |\mathbf{x} - \mathbf{x}_f| \quad , \tag{A.6}$$
$$R_{i||} \equiv \hat{\mathbf{e}} \cdot \mathbf{R}_i \quad , \tag{A.7}$$
$$R_{f||} \equiv \hat{\mathbf{e}} \cdot \mathbf{R}_f \quad , \tag{A.8}$$
$$\mathbf{R}_\perp \equiv \mathbf{R}_i - R_{i||}\hat{\mathbf{e}} \quad , \tag{A.9}$$
$$R_\perp \equiv |\mathbf{R}_\perp| \quad \text{and} \tag{A.10}$$
$$\mathbf{c}(\lambda) \equiv \mathbf{x}_i + \lambda(\mathbf{x}_f - \mathbf{x}_i) \quad \text{for} \quad 0 \leq \lambda \leq 1 \quad . \tag{A.11}$$

The following relations are also needed:

$$L = R_{i||} - R_{f||} \tag{A.12}$$
$$R_i^2 - R_f^2 = L\left(R_{i||} + R_{f||}\right) \tag{A.13}$$
$$\Rightarrow R_{i||} = \frac{R_i^2 - R_f^2}{2L} + \frac{L}{2} \tag{A.14}$$
$$\Rightarrow R_{f||} = \frac{R_i^2 - R_f^2}{2L} - \frac{L}{2} \tag{A.15}$$

Appendix A.1.1. Magnetic Vector Potential

The law of Biot and Savart for the magnetic vector potential of a current density distribution $\mathbf{j}(\mathbf{x})$ is as follows [5]:

$$\mathbf{A}(\mathbf{x}) = \frac{\mu_0}{4\pi} \int \frac{\mathbf{j}(\mathbf{x}')}{|\mathbf{x} - \mathbf{x}'|} \mathrm{d}\mathbf{x}' \quad . \tag{A.16}$$

The parametrization of points on the line segment $\mathbf{c}(\lambda)$ can be used to apply this to the given geometry of a wire segment:

$$\mathbf{A}(\mathbf{x}) = \frac{\mu_0 I}{4\pi} L\hat{\mathbf{e}} \int\limits_0^1 \frac{\mathrm{d}\lambda}{|\mathbf{x} - \mathbf{c}(\lambda)|} \tag{A.17}$$

$$= \frac{\mu_0 I}{4\pi} L\hat{\mathbf{e}} \int\limits_0^1 \frac{\mathrm{d}\lambda}{|\mathbf{x} - \mathbf{x}_i - \lambda L\hat{\mathbf{e}}|} \quad . \tag{A.18}$$

A little bit of geometric intuition is needed to simplify the denominator of the integral:

$$\mathbf{x} - \mathbf{x}_i - \lambda L\hat{\mathbf{e}} = \mathbf{R}_i - \lambda L\hat{\mathbf{e}} \tag{A.19}$$

$$= \mathbf{R}_i - R_{i||}\hat{\mathbf{e}} + R_{i||}\hat{\mathbf{e}} - \lambda L\hat{\mathbf{e}} \tag{A.20}$$

$$= \mathbf{R}_i - R_{i||}\hat{\mathbf{e}} + \left(R_{i||} - \lambda L\right)\hat{\mathbf{e}} \tag{A.21}$$

$$= \mathbf{R}_\perp + \left(R_{i||} - \lambda L\right)\hat{\mathbf{e}} \quad . \tag{A.22}$$

Note that, in particular, $\mathbf{R}_\perp \perp \hat{\mathbf{e}}$ and thus (since $|\hat{\mathbf{e}}| = 1$) due to Pythagoras:

$$|\mathbf{x} - \mathbf{x}_i - \lambda L\hat{\mathbf{e}}|^2 = R_\perp^2 + \left(R_{i||} - \lambda L\right)^2 \tag{A.23}$$

and finally with $R_\perp^2 = R_i^2 - R_{i||}^2$ (also due to Pythagoras):

$$|\mathbf{x} - \mathbf{x}_i - \lambda L\hat{\mathbf{e}}|^2 = R_i^2 - R_{i||}^2 + R_{i||}^2 - 2\lambda L R_{i||} + \lambda^2 L^2 \tag{A.24}$$

$$= R_i^2 - 2\lambda L R_{i||} + \lambda^2 L^2 \quad . \tag{A.25}$$

It follows:

$$\mathbf{A}(\mathbf{x}) = \frac{\mu_0 I}{4\pi} L\hat{\mathbf{e}} \int\limits_0^1 \frac{\mathrm{d}\lambda}{\sqrt{R_i^2 - 2\lambda L R_{i||} + \lambda^2 L^2}} \quad . \tag{A.26}$$

For $X = ax^2 + bx + c$ with $a > 0$ the following relation holds [6]:

$$\int \frac{\mathrm{d}x}{\sqrt{X}} = \frac{1}{\sqrt{a}} \log\left(2\sqrt{aX} + 2ax + b\right) \quad . \tag{A.27}$$

Here, $x = \lambda$, $a = L^2$, $b = -2LR_{i||}$ and $c = R_i^2$. The corresponding antiderivative of the integrand in Eqn. (A.26) is:

$$\int \frac{\mathrm{d}\lambda}{\sqrt{R_i^2 - 2\lambda L R_{i||} + \lambda^2 L^2}} = \frac{1}{L} \log\left(2\sqrt{L^2\left(L^2\lambda^2 - 2LR_{i||}\lambda + R_i^2\right)} + 2L^2\lambda - 2LR_{i||}\right) \quad . \tag{A.28}$$

The definite integral in Eqn. (A.26) is therefore solved by the following expression:

$$\int_0^1 \frac{\mathrm{d}\lambda}{\sqrt{R_i^2 - 2\lambda L R_{i||} + \lambda^2 L^2}} \tag{A.29}$$

$$= \frac{1}{L}\left[\log\left(2\sqrt{L^2\left(L^2 - 2LR_{i||} + R_i^2\right)} + 2L^2 - 2LR_{i||}\right) - \log\left(2\sqrt{L^2 R_i^2} - 2LR_{i||}\right)\right] \tag{A.30}$$

$$= \frac{1}{L}\log\left(\frac{\cancel{2L}\sqrt{L^2 - 2LR_{i||} + R_i^2} + \cancel{2}L^{\cancel{2}} - \cancel{2L}R_{i||}}{\cancel{2L}R_i - \cancel{2L}R_{i||}}\right) \tag{A.31}$$

Note that

$$\begin{aligned} L^2 &= L(R_{i||} - R_{f||}) && \text{(A.32)}\\ &= LR_{i||} - LR_{f||} && \text{(A.33)}\\ \Rightarrow -2LR_{i||} + L^2 &= -\cancel{2}LR_{i||} + \cancel{LR_{i||}} - LR_{f||} && \text{(A.34)}\\ &= -L(R_{i||} + R_{f||}) && \text{(A.35)}\\ &= R_f^2 - R_i^2 && \text{(A.36)}\\ \Rightarrow R_f^2 &= R_i^2 - 2LR_{i||} + L^2 \quad . && \text{(A.37)} \end{aligned}$$

Therefore:

$$\int_0^1 \frac{\mathrm{d}\lambda}{\sqrt{R_i^2 - 2\lambda L R_{i||} + \lambda^2 L^2}} = \frac{1}{L}\log\left(\frac{R_f - R_{f||}}{R_i - R_{i\,\mathrm{d}\varphi||}}\right) \quad . \tag{A.38}$$

Inserting this into Eqn. (A.26) leads to the first intermediate result:

$$\mathbf{A}(\mathbf{x}) = \frac{\mu_0 I}{4\pi}\cancel{L}\frac{1}{\cancel{L}}\log\left(\frac{R_f - R_{f||}}{R_i - R_{i||}}\right)\hat{\mathbf{e}} = \frac{\mu_0 I}{4\pi}\log\left(\frac{R_f - R_{f||}}{R_i - R_{i||}}\right)\hat{\mathbf{e}} \quad . \tag{A.39}$$

However, if the point $\mathbf{x}$ is located on the line extension of the wire segment, $R_i = R_{i||}$ and $R_f = R_{f||}$, which leads to a 0/0 division if this formula is directly evaluated. The solution is to cancel the singular term $(L + R_f - R_i)$, which is also zero for points on the line extension of the wire segment, in the numerator and the denominator of Eqn. (A.39). A second look resolves this:

$$\frac{R_f - R_{f||}}{R_i - R_{i||}} = \frac{2L\left(R_f - R_{f||}\right)}{2L\left(R_i - R_{i||}\right)} = \frac{2LR_f - 2L\left(\frac{R_i^2 - R_f^2}{2L} - \frac{L}{2}\right)}{2LR_i - 2L\left(\frac{R_i^2 - R_f^2}{2L} + \frac{L}{2}\right)} \tag{A.40}$$

$$= \frac{2LR_f - R_i^2 + R_f^2 + L^2}{2LR_i - R_i^2 + R_f^2 - L^2} \tag{A.41}$$

$$= \frac{2LR_f - R_i^2 + R_f^2 + L^2 + LR_i - LR_i + R_iR_f - R_iR_f}{2LR_i - R_i^2 + R_f^2 - L^2 + LR_f - LR_f + R_iR_f - R_iR_f} \tag{A.42}$$

$$= \frac{\cancel{(L + R_f - R_i)}(R_f + R_i + L)}{\cancel{(L + R_f - R_i)}(R_f + R_i - L)} = \frac{R_f + R_i + L}{R_f + R_i - L} \quad . \tag{A.43}$$

It follows for the vector potential expression:

$$\mathbf{A}(\mathbf{x}) = \frac{\mu_0 I}{4\pi} \log\left(\frac{R_f + R_i + L}{R_f + R_i - L}\right) \hat{\mathbf{e}} \quad . \tag{A.44}$$

The authors of Ref. [1] suggest to normalize the length of the wire segment:

$$\frac{R_f + R_i + L}{R_f + R_i - L} = \frac{1+\epsilon}{1-\epsilon} \quad \text{with } \epsilon \equiv \frac{L}{R_i + R_f} \quad , \tag{A.45}$$

leading to

$$\mathbf{A}(\mathbf{x}) = \frac{\mu_0 I}{4\pi} \log\left(\frac{1+\epsilon}{1-\epsilon}\right) \hat{\mathbf{e}} \quad . \tag{A.46}$$

This is the result for the magnetic vector potential of a filamentary wire segment presented in Ref. [1]. However, for $\epsilon \to 0$, the numerical evaluation of this expression is problematic. It is therefore suggested to use the following expression, which works for points extremely close to, extremely far away from and all in-between locations with respect to the wire segment. Note that

$$\operatorname{artanh}(\epsilon) = \frac{1}{2} \log\left(\frac{1+\epsilon}{1-\epsilon}\right) \quad , \tag{A.47}$$

leading to

$$\boxed{\mathbf{A}(\mathbf{x}) = \frac{\mu_0 I}{2\pi} \operatorname{artanh}(\epsilon)\, \hat{\mathbf{e}}} \quad . \tag{A.48}$$

Appendix A.1.2. Magnetic Field

The magnetic field $\mathbf{B}(\mathbf{x})$ is computed from $\mathbf{B} = \nabla \times \mathbf{A}$, applied to Eqn. (A.46). Define

$$f(\epsilon) \equiv \log\left(\frac{1+\epsilon}{1-\epsilon}\right) \tag{A.49}$$

and it follows:

$$\frac{4\pi}{\mu_0 I}\mathbf{B} = \nabla \times (f(\epsilon)\hat{\mathbf{e}}) = \nabla f(\epsilon) \times \hat{\mathbf{e}} + f(\epsilon)\underbrace{\nabla \times \hat{\mathbf{e}}}_{=0} = f'(\epsilon)\nabla\epsilon \times \hat{\mathbf{e}} \quad . \tag{A.50}$$

Note that

$$\nabla\epsilon = \nabla\left(\frac{L}{R_i + R_f}\right) = \frac{-L}{(R_i+R_f)^2}\left(\nabla R_i + \nabla R_f\right) = \frac{-L}{(R_i+R_f)^2}\left(\frac{\mathbf{R}_i}{R_i} + \frac{\mathbf{R}_f}{R_f}\right) \quad . \tag{A.51}$$

It follows:

$$\frac{4\pi}{\mu_0 I}\mathbf{B} = f'(\epsilon)\frac{-L}{(R_i+R_f)^2}\left(\frac{\mathbf{R}_i}{R_i} + \frac{\mathbf{R}_f}{R_f}\right) \times \hat{\mathbf{e}} \tag{A.52}$$

$$= f'(\epsilon)\frac{L}{(R_i+R_f)^2}\,\hat{\mathbf{e}} \times \left(\frac{\mathbf{R}_i}{R_i} + \frac{\mathbf{R}_f}{R_f}\right) \tag{A.53}$$

$$= f'(\epsilon)\frac{\epsilon^2}{L}\,\hat{\mathbf{e}} \times \left(\frac{\mathbf{R}_i}{R_i} + \frac{\mathbf{R}_f}{R_f}\right) \quad . \tag{A.54}$$

Also:

$$\frac{\mathbf{R}_i}{R_i} + \frac{\mathbf{R}_f}{R_f} = \frac{\mathbf{R}_i}{R_i} + \frac{\mathbf{R}_i - L\hat{\mathbf{e}}}{R_f} = \frac{R_f\mathbf{R}_i + R_i(\mathbf{R}_i - L\hat{\mathbf{e}})}{R_iR_f} = \frac{(R_f + R_i)\mathbf{R}_i + R_iL\hat{\mathbf{e}}}{R_iR_f} \tag{A.55}$$

$$= \frac{R_f + R_i}{R_iR_f}\mathbf{R}_i + \frac{R_iL}{R_iR_f}\,\hat{\mathbf{e}} \tag{A.56}$$

and therefore:

$$\hat{\mathbf{e}}\times\left(\frac{\mathbf{R}_i}{R_i} + \frac{\mathbf{R}_f}{R_f}\right) = \hat{\mathbf{e}}\times\left(\frac{R_f + R_i}{R_iR_f}\mathbf{R}_i + \frac{R_iL}{R_iR_f}\,\hat{\mathbf{e}}\right) = \frac{R_f + R_i}{R_iR_f}\,\hat{\mathbf{e}}\times\mathbf{R}_i \quad , \tag{A.57}$$

since $\hat{\mathbf{e}} \times \hat{\mathbf{e}} = 0$. Inserting this into Eqn. (A.54) leads to:

$$\frac{4\pi}{\mu_0 I}\mathbf{B} = f'(\epsilon)\frac{\epsilon^{\cancel{2}}}{\cancel{L}}\,\frac{\cancel{R_f + R_i}}{R_iR_f}\,\hat{\mathbf{e}} \times \mathbf{R}_i = f'(\epsilon)\frac{\epsilon}{R_iR_f}\,\hat{\mathbf{e}} \times \mathbf{R}_i \tag{A.58}$$

Next, look at $f'(\epsilon)$:

$$f'(\epsilon) = \frac{\cancel{1-\epsilon}}{1+\epsilon} \cdot \frac{1(1-\epsilon)-(1+\epsilon)(-1)}{(1-\epsilon)^{\cancel{2}}} = \frac{1-\epsilon+1+\epsilon}{(1+\epsilon)(1-\epsilon)} = \frac{2}{1-\epsilon^2} \tag{A.59}$$

and insert this into Eqn. (A.58):

$$\frac{4\pi}{\mu_0 I}\mathbf{B} = \frac{2\epsilon}{1-\epsilon^2} \cdot \frac{1}{R_i R_f}\, \hat{\mathbf{e}} \times \mathbf{R}_i \tag{A.60}$$

$$= \frac{2L}{\cancel{R_i + R_f}} \cdot \frac{(R_i+R_f)^{\cancel{2}}}{(R_i+R_f)^2 - L^2} \cdot \frac{1}{R_i R_f}\, \hat{\mathbf{e}} \times \mathbf{R}_i \quad . \tag{A.61}$$

This results in the final expression for the magnetic field:

$$\boxed{\mathbf{B}(\mathbf{x}) = \frac{\mu_0 I}{4\pi} \frac{2L(R_i+R_f)}{R_i R_f} \frac{1}{(R_i+R_f)^2 - L^2}\, \hat{\mathbf{e}} \times \mathbf{R}_i} \quad . \tag{A.62}$$

Appendix A.2. Circular Wire Loop

The current density of the wire loop can be expressed as follows:

$$\mathbf{j}(\mathbf{x}') = I\delta(\rho' - a)\delta(z')\, \hat{\mathbf{e}}_{\varphi'}\,. \tag{A.63}$$

Appendix A.2.1. Magnetic Vector Potential

The Biot-Savart law for the magnetic vector potential reads:

$$\begin{aligned}
\mathbf{A}(\mathbf{x}) &= \frac{\mu_0}{4\pi} \int_{\mathbb{R}^3} \frac{\mathbf{j}(\mathbf{x}')}{|\mathbf{x}-\mathbf{x}'|}\, \mathrm{d}^3\mathbf{x}' \\
&= \frac{\mu_0 I}{4\pi} \int_{\mathbb{R}^3} \frac{\delta(\rho'-a)\delta(z')}{|\mathbf{x}-\mathbf{x}'|}\, \hat{\mathbf{e}}_{\varphi'}\, \mathrm{d}^3\mathbf{x}' \\
&= \frac{\mu_0 I}{4\pi} \int\limits_{-\infty}^{\infty} \int\limits_{0}^{2\pi} \int\limits_{0}^{\infty} \frac{\delta(\rho'-a)\delta(z')}{|\mathbf{x}-\mathbf{x}'|}\, \hat{\mathbf{e}}_{\varphi'} \rho'\, \mathrm{d}\rho'\, \mathrm{d}\varphi'\, \mathrm{d}z'
\end{aligned} \tag{A.64}$$

where a change of variables from Cartesian coordinates to cylindrical coordinates was performed in the integral. The differential volume element was adjusted according to $\mathrm{d}^3\mathbf{x}' = \rho'\, \mathrm{d}\rho'\, \mathrm{d}\varphi'\, \mathrm{d}z'$. The coordinate system is rotated around the z axis to yield $\varphi = 0$ for the evaluation location $\mathbf{x}$ which is generally acceptable due to the rotational symmetry of the circular wire loop. Then, $\mathbf{x} = (x, y, z)$ in Cartesian coordinates with

$$x = \rho\cos(\varphi) = \rho \tag{A.65}$$

$$y = \rho\sin(\varphi) = 0\,. \tag{A.66}$$

The distance $|\mathbf{x}-\mathbf{x}'|$ is then:

$$\begin{aligned}|\mathbf{x}-\mathbf{x}'| &= \sqrt{(\rho-\rho'\cos(\varphi'))^2+\rho'^2\sin^2(\varphi')+(z-z')^2}\\ &= \sqrt{\rho^2+\rho'^2(\cos(\varphi'))^2+\sin^2(\varphi'))-2\rho\rho'\cos(\varphi')+(z-z')^2}\\ &= \sqrt{\rho^2+\rho'^2+(z-z')^2-2\rho\rho'\cos(\varphi')}\,. \end{aligned} \tag{A.67}$$

Inserting this into Eqn. (A.64) leads to:

$$\mathbf{A}(\mathbf{x}) = \frac{\mu_0 I}{4\pi}\int\limits_{-\infty}^{\infty}\int\limits_{0}^{2\pi}\int\limits_{0}^{\infty}\frac{\delta(\rho'-a)\delta(z')}{\sqrt{\rho^2+\rho'^2+(z-z')^2-2\rho\rho'\cos(\varphi')}}\,\hat{\mathbf{e}}_{\varphi'}\rho'\,\mathrm{d}\rho'\,\mathrm{d}\varphi'\,\mathrm{d}z' \tag{A.68}$$

and the integrals over ρ' and z' can be evaluated already:

$$\mathbf{A}(\mathbf{x}) = \frac{\mu_0 I a}{4\pi}\int\limits_{0}^{2\pi}\frac{\hat{\mathbf{e}}_{\varphi'}\,\mathrm{d}\varphi'}{\sqrt{\rho^2+a^2+z^2-2\rho a\cos(\varphi')}}\,. \tag{A.69}$$

The cylindrical components of the magnetic vector potential $\mathbf{A}$ are obtained by dotting above result with the cylindrical unit vector at the evaluation location $\mathbf{x}$:

$$\mathbf{A}(\mathbf{x}) = A_\rho\,\hat{\mathbf{e}}_\rho + A_\varphi\,\hat{\mathbf{e}}_\varphi + A_z\,\hat{\mathbf{e}}_z \tag{A.70}$$

with

$$A_\rho = \mathbf{A}(\mathbf{x})\cdot\,\hat{\mathbf{e}}_\rho \tag{A.71}$$

$$A_\varphi = \mathbf{A}(\mathbf{x})\cdot\,\hat{\mathbf{e}}_\varphi \tag{A.72}$$

$$A_z = \mathbf{A}(\mathbf{x})\cdot\,\hat{\mathbf{e}}_z\,. \tag{A.73}$$

The dot products of the cylindrical unit vectors are:

$$\hat{\mathbf{e}}_{\varphi'} \cdot \hat{\mathbf{e}}_\rho = \begin{pmatrix} -\sin(\varphi') \\ \cos(\varphi') \\ 0 \end{pmatrix} \cdot \begin{pmatrix} \cos(\varphi) \\ \sin(\varphi) \\ 0 \end{pmatrix} = \begin{pmatrix} -\sin(\varphi') \\ \cos(\varphi') \\ 0 \end{pmatrix} \cdot \begin{pmatrix} 1 \\ 0 \\ 0 \end{pmatrix} = -\sin(\varphi') \tag{A.74}$$

$$\hat{\mathbf{e}}_{\varphi'} \cdot \hat{\mathbf{e}}_\varphi = \begin{pmatrix} -\sin(\varphi') \\ \cos(\varphi') \\ 0 \end{pmatrix} \cdot \begin{pmatrix} -\sin(\varphi) \\ \cos(\varphi) \\ 0 \end{pmatrix} = \begin{pmatrix} -\sin(\varphi') \\ \cos(\varphi') \\ 0 \end{pmatrix} \cdot \begin{pmatrix} 0 \\ 1 \\ 0 \end{pmatrix} = \cos(\varphi') \tag{A.75}$$

$$\hat{\mathbf{e}}_{\varphi'} \cdot \hat{\mathbf{e}}_z = \begin{pmatrix} -\sin(\varphi') \\ \cos(\varphi') \\ 0 \end{pmatrix} \cdot \begin{pmatrix} 0 \\ 0 \\ 1 \end{pmatrix} = 0\,. \tag{A.76}$$

The expression from Eqn. (A.69) is inserted into above expressions. The vertical component A_z vanishes trivially since the unit vectors are orthogonal, as can be seen from Eqn. (A.76). For the radial component A_ρ it follows:

$$A_\rho = \frac{\mu_0 I a}{4\pi} \int_0^{2\pi} \frac{-\sin(\varphi')\,\mathrm{d}\varphi'}{\sqrt{\rho^2 + a^2 + z^2 - 2\rho a \cos(\varphi')}} = 0\,, \tag{A.77}$$

since the integrand is an odd function of φ'. The tangential component A_φ is non-zero because the integrand is an even function of φ'. It is given by:

$$A_\varphi(\rho, z) = \frac{\mu_0 I a}{4\pi} \int_0^{2\pi} \frac{\cos(\varphi')\,\mathrm{d}\varphi'}{\sqrt{\rho^2 + a^2 + z^2 - 2\rho a \cos(\varphi')}}\,, \tag{A.78}$$

leading to

$$\mathbf{A}(\mathbf{x}) = A_\varphi(\rho, z)\,\hat{\mathbf{e}}_\varphi\,. \tag{A.79}$$

A change of variables from φ' to β is performed in order to solve Eqn. (A.78):

$$\varphi' = 2\beta + \pi \tag{A.80}$$

which implies

$$\frac{\mathrm{d}\varphi'}{\mathrm{d}\beta} = 2 \Rightarrow \mathrm{d}\varphi' = 2\mathrm{d}\beta \tag{A.81}$$

$$\varphi'_0 = 0 \Rightarrow \beta_0 = -\frac{\pi}{2} \tag{A.82}$$

$$\varphi'_1 = 2\pi \Rightarrow \beta_1 = \frac{\pi}{2}\,. \tag{A.83}$$

It follows for Eqn. (A.78):

$$A_\varphi(\rho, z) = \frac{\mu_0 I a}{4\pi} \int\limits_{-\pi/2}^{\pi/2} \frac{2\cos(2\beta + \pi)\,\mathrm{d}\beta}{\sqrt{\rho^2 + a^2 + z^2 - 2\rho a\cos(2\beta + \pi)}}\,. \tag{A.84}$$

Note that $\cos(2\beta + \pi) = -\cos(2\beta)$:

$$A_\varphi(\rho, z) = \frac{\mu_0 I a}{2\pi} \int\limits_{-\pi/2}^{\pi/2} \frac{-\cos(2\beta)\,\mathrm{d}\beta}{\sqrt{\rho^2 + a^2 + z^2 + 2\rho a\cos(2\beta)}}\,. \tag{A.85}$$

In the numerator of the integrand it follows:

$$-\cos(2\beta) = -\left(\cos^2(\beta) - \sin^2(\beta)\right) = \sin^2(\beta) - \cos^2(\beta)\,. \tag{A.86}$$

The denominator of the integrand can be reformulated by introducing normalized coordinates $\rho' = \rho/a$ and $z' = z/a$ as follows:

$$\begin{aligned}
&\rho^2 + a^2 + z^2 + 2\rho a\cos(2\beta) \\
&= a^2\left[z'^2 + \rho'^2 + 1 + 2\rho'\cos(2\beta)\right] \\
&= a^2\left[z'^2 + (1+\rho')^2 - 2\rho' + 2\rho'\cos(2\beta)\right] \\
&= a^2\left[z'^2 + (1+\rho')^2 - 2\rho'\left(1 - \cos(2\beta)\right)\right] \\
&= a^2\left[z'^2 + (1+\rho')^2 - 2\rho'\left(1 + \sin^2(\beta) - \cos^2(\beta)\right)\right] \\
&= a^2\left[z'^2 + (1+\rho')^2 - 2\rho'\left(\cancel{\cos^2(\beta)} + \sin^2(\beta) + \sin^2(\beta) \cancel{- \cos^2(\beta)}\right)\right] \\
&= a^2\left[z'^2 + (1+\rho')^2 - 4\rho'\sin^2(\beta)\right] \\
&= a^2\left(z'^2 + (1+\rho')^2\right)\left[1 - \underbrace{\frac{4\rho'}{z'^2 + (1+\rho')^2}}_{\equiv k^2}\sin^2(\beta)\right] \\
&= a^2\left(z'^2 + (1+\rho')^2\right)\left[1 - k^2\sin^2(\beta)\right]
\end{aligned} \tag{A.87}$$

with

$$k^2 = \frac{4\rho'}{z'^2 + (1+\rho')^2}\,. \tag{A.88}$$

Inserting this into Eqn. (A.85) leads to:

$$A_\varphi(\rho', z') = \frac{\mu_0 I}{2\pi} \frac{1}{\sqrt{z'^2 + (1+\rho')^2}} \int\limits_{-\pi/2}^{\pi/2} \frac{\sin^2(\beta) - \cos^2(\beta)}{\sqrt{1 - k^2\sin^2(\beta)}}\,\mathrm{d}\beta\,. \tag{A.89}$$

Focusing again on the denominator of the integrand:

$$\begin{aligned}
1 - k^2 \sin^2(\beta) &= \cos^2(\beta) + \sin^2(\beta) - \frac{4\rho'}{z'^2 + (1+\rho')^2} \sin^2(\beta) \\
&= \cos^2(\beta) + \left(1 - \frac{4\rho'}{z'^2 + (1+\rho')^2}\right) \sin^2(\beta) \\
&= \cos^2(\beta) + \frac{z'^2 + (1+\rho')^2 - 4\rho'}{z'^2 + (1+\rho')^2} \sin^2(\beta) \\
&= \cos^2(\beta) + \underbrace{\frac{z'^2 + (1-\rho')^2}{z'^2 + (1+\rho')^2}}_{\equiv k_c^2} \sin^2(\beta) \\
&= \cos^2(\beta) + k_c^2 \sin^2(\beta) \qquad \text{(A.90)}
\end{aligned}$$

with

$$k_c^2 = \frac{z'^2 + (1-\rho')^2}{z'^2 + (1+\rho')^2}\,, \qquad \text{(A.91)}$$

leading to:

$$A_\varphi(\rho', z') = \frac{\mu_0 I}{2\pi} \frac{1}{\sqrt{z'^2 + (1+\rho')^2}} \int\limits_{-\pi/2}^{\pi/2} \frac{\sin^2(\beta) - \cos^2(\beta)}{\sqrt{\cos^2(\beta) + k_c^2 \sin^2(\beta)}} \, \mathrm{d}\beta\,. \qquad \text{(A.92)}$$

The integrand is symmetric about 0 and therefore the integration domain can be halved if a factor of 2 is included:

$$A_\varphi(\rho', z') = \frac{\mu_0 I}{\pi} \frac{1}{\sqrt{z'^2 + (1+\rho')^2}} \int\limits_{0}^{\pi/2} \frac{\sin^2(\beta) - \cos^2(\beta)}{\sqrt{\cos^2(\beta) + k_c^2 \sin^2(\beta)}} \, \mathrm{d}\beta\,. \qquad \text{(A.93)}$$

The remaining integral is a complete elliptic integral which can be expressed using the form introduced by Bulirsch [7]:

$$\mathrm{cel}(k_c, p, a, b) = \int\limits_{0}^{\pi/2} \frac{a\cos^2(\varphi) + b\sin^2(\varphi)}{\cos^2(\varphi) + p\sin^2(\varphi)} \frac{\mathrm{d}\varphi}{\sqrt{\cos^2(\varphi) + k_c^2 \sin^2(\varphi)}}\,. \qquad \text{(A.94)}$$

Note that the parameter a of $\mathrm{cel}(k_c, p, a, b)$ is not to be confused with the radius of the wire loop. A numerical implementation of the general complete elliptic integral $\mathrm{cel}(k_c, p, a, b)$ is provided in the cited article. The use of this particular implementation is inspired by Ref. [8]. Putting above results together, we arrive at the following expression for A_φ:

$$\boxed{A_\varphi(\rho', z') = \frac{\mu_0 I}{\pi} \frac{1}{\sqrt{z'^2 + (1+\rho')^2}} \,\mathrm{cel}(k_c, 1, -1, 1)}\,. \tag{A.95}$$

In Eqn. (5.37) of Ref. [5] the tangential component is given by:

$$A_\varphi(r, \theta) = \frac{\mu_0}{4\pi} \frac{4Ia}{\sqrt{a^2 + r^2 + 2ar\sin(\theta)}} \left[\frac{(2-k^2)K(k) - 2E(k)}{k^2}\right] \tag{A.96}$$

with

$$k^2 = \frac{4ar\sin(\theta)}{a^2 + r^2 + 2ar\sin(\theta)}\,. \tag{A.97}$$

Here, $K(k)$ and $E(k)$ are the complete elliptic integrals of the first and second kind, respectively. Spherical coordinates are used with $r\sin(\theta) = \rho$ and $r^2 = \rho^2 + z^2$. In order to bring this to the form in Eqn. (A.95), an expression for the linear combination of $K(k)$ and $E(k)$ from Ref. [7] is used:

$$\lambda K(k) + \mu E(k) = \mathrm{cel}(k_c, 1, \lambda + \mu, \lambda + \mu k_c^2) \tag{A.98}$$

where

$$k^2 + k_c^2 = 1\,. \tag{A.99}$$

The argument of the elliptic integrals is considered first:

$$\begin{aligned}
k^2 &= \frac{4ar\sin(\theta)}{a^2 + r^2 + 2ar\sin(\theta)} = \frac{4a\rho}{a^2 + r^2 + 2a\rho} = \frac{4\cancel{a}\rho}{a^{\cancel{2}}\left(1 + \frac{r^2}{a^2} + 2\frac{\rho}{a}\right)} \\
&= \frac{4\rho'}{1 + \frac{r^2}{a^2} + 2\rho'} = 4\rho'\left(1 + \frac{\rho^2 + z^2}{a^2} + 2\rho'\right)^{-1} = 4\rho'\left(1 + \rho'^2 + z'^2 + 2\rho'\right)^{-1} \\
&= \frac{4\rho'}{z'^2 + (1+\rho')^2}\,.
\end{aligned} \tag{A.100}$$

Thus, k^2 from Ref. [5] is equivalent to k^2 in Eqn. (A.88). Inserting this into Eqn. (A.96) leads to:

$$\begin{aligned}
A_\varphi(r, \theta) &= \frac{\mu_0 I}{\cancel{2}\pi} \frac{\cancel{2}}{\sqrt{z'^2 + (1+\rho')^2}} \left[\frac{(2-k^2)K(k) - 2E(k)}{k^2}\right] \\
&= \frac{\mu_0 I}{\pi} \frac{1}{\sqrt{z'^2 + (1+\rho')^2}} \left[\frac{(2-k^2)K(k) - 2E(k)}{k^2}\right]\,.
\end{aligned} \tag{A.101}$$

The coefficients of the elliptic integrals are given as follows:

$$\lambda = \frac{2-k^2}{k^2} = \frac{2}{k^2} - 1 \tag{A.102}$$

$$\mu = -\frac{2}{k^2} \tag{A.103}$$

and their combinations are as follows:

$$\lambda + \mu = \frac{2}{k^2} - 1 - \frac{2}{k^2} = -1 \tag{A.104}$$

$$\begin{aligned} \lambda + \mu k_c^2 &= \frac{2}{k^2} - 1 - \frac{2}{k^2}(1-k^2) \\ &= \frac{2}{k^2} - 1 - \frac{2}{k^2} + 2 = 1\,. \end{aligned} \tag{A.105}$$

Putting above results together, we arrive at the following expression for A_φ:

$$\boxed{A_\varphi(r,\theta) = \frac{\mu_0 I}{\pi} \frac{1}{\sqrt{z'^2 + (1+\rho')^2}} \operatorname{cel}(k_c, 1, -1, 1)} \tag{A.106}$$

with $\rho' = r/a \sin(\theta)$, $z' = \sqrt{r^2 - \rho^2}/a$ and k_c given by Eqn. (A.91)). It is favorable for numerical evaluation of A_φ to use the form given in Eqn. (A.95) where the linear combination of the complete elliptic integrals is embedded in the parameters of $\operatorname{cel}(k_c, p, a, b)$ and no precautions need to be taken to deal with cancellations in Eqn. (A.96).

Appendix A.2.2. Magnetic Field

The magnetic field is computed using $\mathbf{B} = \nabla \times \mathbf{A}$. In cylindrical coordinates with the form of the magnetic vector potential from Eqn. (A.79) the curl is given as follows:

$$\mathbf{B}(\mathbf{x}) = B_\rho \hat{\mathbf{e}}_\rho + B_z \hat{\mathbf{e}}_z \tag{A.107}$$

with

$$B_\rho = -\frac{\partial A_\varphi}{\partial z} \tag{A.108}$$

$$B_z = \frac{1}{\rho}\frac{\partial(\rho A_\varphi)}{\partial \rho} = \frac{A_\varphi}{\rho} + \frac{\partial A_\varphi}{\partial \rho}\,. \tag{A.109}$$

Starting from Eqn. (A.78) it is noted that the partial derivatives only act on the denominator of the integrand. Therefore, consider first:

$$\begin{aligned}
\frac{\partial}{\partial z}\left(a^2+z^2+\rho^2-2a\rho\cos(\varphi)\right)^{-\frac{1}{2}} &= -\frac{\cancel{1}}{\cancel{2}}\left(a^2+z^2+\rho^2-2a\rho\cos(\varphi)\right)^{-\frac{3}{2}}(\cancel{2}z) \\
&= \frac{-z}{\left[a^2+z^2+\rho^2-2a\rho\cos(\varphi)\right]^{\frac{3}{2}}} \qquad \text{(A.110)} \\
\frac{\partial}{\partial \rho}\left(a^2+z^2+\rho^2-2a\rho\cos(\varphi)\right)^{-\frac{1}{2}} &= -\frac{\cancel{1}}{\cancel{2}}\left(a^2+z^2+\rho^2-2a\rho\cos(\varphi)\right)^{-\frac{3}{2}}(\cancel{2}\rho-\cancel{2}a\cos(\varphi)) \\
&= \frac{-(\rho-a\cos(\varphi))}{\left[a^2+z^2+\rho^2-2a\rho\cos(\varphi)\right]^{\frac{3}{2}}} . \qquad \text{(A.111)}
\end{aligned}$$

These expressions are used to formulate Eqn. (A.108) and a change of variables from φ to β analogously to the step from Eqn. (A.78) to Eqn. (A.85) is performed. Finally, normalized coordinates are introduced in the integrand similar to the steps from Eqn. (A.87) to Eqn. (A.90):

$$\begin{aligned}
B_\rho &= \frac{\partial}{\partial z}\left(\frac{\mu_0 I a}{4\pi}\int_0^{2\pi}\frac{\cos(\varphi')\,\mathrm{d}\varphi'}{\sqrt{\rho^2+a^2+z^2-2\rho a\cos(\varphi')}}\right) \\
&= -\frac{\mu_0 I a z}{4\pi}\int_0^{2\pi}\frac{\cos(\varphi')\,\mathrm{d}\varphi'}{\left[a^2+z^2+\rho^2-2a\rho\cos(\varphi')\right]^{\frac{3}{2}}} \\
&= \frac{\mu_0 I a z}{2\pi}\int_{-\pi/2}^{\pi/2}\frac{\cos(2\beta)\,\mathrm{d}\beta}{\left[a^2+z^2+\rho^2+2a\rho\cos(2\beta)\right]^{\frac{3}{2}}} \\
&= \frac{\mu_0 I}{2\pi}\frac{\cancel{a^2}z'}{a^{\cancel{3}}\left(z'^2+(1+\rho')^2\right)^{\frac{3}{2}}}\int_{-\pi/2}^{\pi/2}\frac{\sin^2(\beta)-\cos^2(\beta)}{\left[\cos^2(\beta)+k_c^2\sin^2(\beta)\right]^{\frac{3}{2}}}\,\mathrm{d}\beta \qquad \text{(A.112)}
\end{aligned}$$

This integrand is also symmetric about 0, which can be used to express Eqn. (A.112) in terms of the general complete elliptic integral:

$$\boxed{B_\rho(\rho', z') = \frac{\mu_0 I}{\pi a}\frac{z'}{\left[z'^2+(1+\rho')^2\right]^{\frac{3}{2}}}\,\mathrm{cel}(k_c, k_c^2, -1, 1)} . \qquad \text{(A.113)}$$

Regarding B_z the first term in Eqn. (A.109) can already be written down using $\rho = a\rho'$ and A_φ from Eqn. (A.95):

$$B_z = \frac{\mu_0 I}{\pi a} \frac{1}{\rho' \sqrt{z'^2 + (1+\rho')^2}} \operatorname{cel}(k_c, 1, -1, 1) + \frac{\partial A_\varphi}{\partial \rho} \tag{A.114}$$

The second term is considered next:

$$\begin{aligned}
\frac{\partial A_\varphi}{\partial \rho} &= \frac{\partial A_\varphi}{\partial \rho'} \frac{\partial \rho'}{\partial \rho} = \frac{1}{a} \frac{\partial A_\varphi}{\partial \rho'} \\
&= \frac{1}{a} \frac{\partial}{\partial \rho'} \left[\frac{\mu_0 I}{\pi} \frac{1}{\sqrt{z'^2 + (1+\rho')^2}} \operatorname{cel}(k_c, 1, -1, 1) \right] \\
&= \frac{\mu_0 I}{\pi a} \frac{\partial}{\partial \rho'} \left[\frac{1}{\sqrt{z'^2 + (1+\rho')^2}} \operatorname{cel}(k_c, 1, -1, 1) \right] \\
&= \frac{\mu_0 I}{\pi a} \Bigg\{ \quad \frac{\partial}{\partial \rho'} \left[\frac{1}{\sqrt{z'^2 + (1+\rho')^2}} \right] \operatorname{cel}(k_c, 1, -1, 1) \\
&\qquad\qquad + \frac{1}{\sqrt{z'^2 + (1+\rho')^2}} \frac{\partial}{\partial \rho'} \operatorname{cel}(k_c, 1, -1, 1) \Bigg\} \\
&= \frac{\mu_0 I}{\pi a} \Bigg\{ \quad \frac{-(1+\rho')}{\left[z'^2 + (1+\rho')^2\right]^{3/2}} \operatorname{cel}(k_c, 1, -1, 1) \\
&\qquad\qquad + \frac{1}{\sqrt{z'^2 + (1+\rho')^2}} \frac{\partial (k_c^2)}{\partial \rho'} \frac{\partial}{\partial (k_c^2)} \operatorname{cel}(k_c, 1, -1, 1) \Bigg\}.
\end{aligned} \tag{A.115}$$

Consider the remaining derivatives:

$$\begin{aligned}
\frac{\partial (k_c^2)}{\partial \rho'} &= \frac{\partial}{\partial \rho'} \left(\frac{z'^2 + (1-\rho')^2}{z'^2 + (1+\rho')^2} \right) \\
&= \frac{1}{z'^2 + (1+\rho')^2} \left(-2(1-\rho') - k_c^2\, 2(1+\rho') \right) \\
&= \frac{-2}{z'^2 + (1+\rho')^2} \left(1 - \rho' + k_c^2 (1+\rho') \right) \\
&= \frac{-2}{z'^2 + (1+\rho')^2} \left(1 + k_c^2 - (1-k_c^2)\rho' \right)
\end{aligned} \tag{A.116}$$

as well as:

$$
\begin{aligned}
&\frac{\partial}{\partial(k_c^2)}\,\mathrm{cel}(k_c,1,-1,1)\\
&\quad=\frac{\partial}{\partial(k_c^2)}\int\limits_0^{\pi/2}\frac{\sin^2(\varphi)-\cos^2(\varphi)}{\sqrt{\cos^2(\varphi)+k_c^2\sin^2(\varphi)}}\,\mathrm{d}\varphi\\
&\quad=\int\limits_0^{\pi/2}\left[\sin^2(\varphi)-\cos^2(\varphi)\right]\frac{\partial}{\partial(k_c^2)}\left[\cos^2(\varphi)+k_c^2\sin^2(\varphi)\right]^{-1/2}\,\mathrm{d}\varphi\\
&\quad=\int\limits_0^{\pi/2}\left[\sin^2(\varphi)-\cos^2(\varphi)\right]\left(-\frac{1}{2}\right)\left[\cos^2(\varphi)+k_c^2\sin^2(\varphi)\right]^{-3/2}\sin^2(\varphi)\,\mathrm{d}\varphi\\
&\quad=-\frac{1}{2}\int\limits_0^{\pi/2}\frac{\left[\sin^2(\varphi)-\cos^2(\varphi)\right]\sin^2(\varphi)}{\left[\cos^2(\varphi)+k_c^2\sin^2(\varphi)\right]^{3/2}}\,\mathrm{d}\varphi\,. \qquad \text{(A.117)}
\end{aligned}
$$

These terms are now inserted into Eqn. (A.115):

$$
\begin{aligned}
\frac{\partial A_\varphi}{\partial\rho}=\frac{\mu_0 I}{\pi a}\Bigg\{\;&\frac{-(1+\rho')}{\left[z'^2+(1+\rho')^2\right]^{3/2}}\,\mathrm{cel}(k_c,1,-1,1)\\
&+\frac{1}{\sqrt{z'^2+(1+\rho')^2}}\frac{\cancel{-2}}{z'^2+(1+\rho')^2}\left(1+k_c^2-(1-k_c^2)\rho'\right)\\
&\cancel{\left(-\frac{1}{2}\right)}\int\limits_0^{\pi/2}\frac{\left[\sin^2(\varphi)-\cos^2(\varphi)\right]\sin^2(\varphi)}{\left[\cos^2(\varphi)+k_c^2\sin^2(\varphi)\right]^{3/2}}\,\mathrm{d}\varphi\Bigg\}\\
=\frac{\mu_0 I}{\pi a}\Bigg\{\;&\frac{-(1+\rho')}{\left[z'^2+(1+\rho')^2\right]^{3/2}}\,\mathrm{cel}(k_c,1,-1,1)\\
&+\frac{1+k_c^2-(1-k_c^2)\rho'}{\left[z'^2+(1+\rho')^2\right]^{3/2}}\int\limits_0^{\pi/2}\frac{\left[\sin^2(\varphi)-\cos^2(\varphi)\right]\sin^2(\varphi)}{\left[\cos^2(\varphi)+k_c^2\sin^2(\varphi)\right]^{3/2}}\,\mathrm{d}\varphi\Bigg\}\,.
\end{aligned}
\qquad \text{(A.118)}
$$

This form of $\partial A_\varphi/\partial\rho$ is now inserted into Eqn. (A.114). $\partial A_\varphi/\partial\rho$ has to be multiplied by a factor of ρ' in order to factor out a common prefactor $1/\rho'$.

This leads to:

$$
\begin{aligned}
B_z = {}& \frac{\mu_0 I}{\pi a} \frac{1}{\rho' \sqrt{z'^2 + (1+\rho')^2}} \left\{ \operatorname{cel}(k_c, 1, -1, 1) - \frac{\rho'(1+\rho')}{z'^2 + (1+\rho')^2} \operatorname{cel}(k_c, 1, -1, 1) \right. \\
& \left. + \frac{\rho' \left[1 + k_c^2 - (1-k_c^2)\rho'\right]}{z'^2 + (1+\rho')^2} \int_0^{\pi/2} \frac{\left[\sin^2(\varphi) - \cos^2(\varphi)\right] \sin^2(\varphi)}{\left[\cos^2(\varphi) + k_c^2 \sin^2(\varphi)\right]^{3/2}} \, \mathrm{d}\varphi \right\} \\
= {}& \frac{\mu_0 I}{\pi a} \frac{1}{\rho' \sqrt{z'^2 + (1+\rho')^2}} \left\{ \left(1 - \frac{\rho'(1+\rho')}{z'^2 + (1+\rho')^2}\right) \operatorname{cel}(k_c, 1, -1, 1) \right. \\
& \left. + \frac{\rho' \left[1 + k_c^2 - (1-k_c^2)\rho'\right]}{z'^2 + (1+\rho')^2} \int_0^{\pi/2} \frac{\left[\sin^2(\varphi) - \cos^2(\varphi)\right] \sin^2(\varphi)}{\left[\cos^2(\varphi) + k_c^2 \sin^2(\varphi)\right]^{3/2}} \, \mathrm{d}\varphi \right\} \\
= {}& \frac{\mu_0 I}{\pi a} \frac{1}{\rho' \sqrt{z'^2 + (1+\rho')^2}} \left\{ \left(1 - \frac{\rho'(1+\rho')}{z'^2 + (1+\rho')^2}\right) \int_0^{\pi/2} \frac{\sin^2(\varphi) - \cos^2(\varphi)}{\sqrt{\cos^2(\varphi) + k_c^2 \sin^2(\varphi)}} \, \mathrm{d}\varphi \right. \\
& \left. + \frac{\rho' \left[1 + k_c^2 - (1-k_c^2)\rho'\right]}{z'^2 + (1+\rho')^2} \int_0^{\pi/2} \frac{\left[\sin^2(\varphi) - \cos^2(\varphi)\right] \sin^2(\varphi)}{\left[\cos^2(\varphi) + k_c^2 \sin^2(\varphi)\right]^{3/2}} \, \mathrm{d}\varphi \right\} .
\end{aligned}
\tag{A.119}
$$

The integrand of the two integrals can be combined. A nutritious one needs to be included in the first integrand:

$$
\begin{aligned}
B_z = {}& \frac{\mu_0 I}{\pi a} \frac{1}{\rho' \sqrt{z'^2 + (1+\rho')^2}} \int_0^{\pi/2} \mathrm{d}\varphi \, \frac{\sin^2(\varphi) - \cos^2(\varphi)}{\left[\cos^2(\varphi) + k_c^2 \sin^2(\varphi)\right]^{3/2}} \\
& \left\{ \left(1 - \frac{\rho'(1+\rho')}{z'^2 + (1+\rho')^2}\right) \left[\cos^2(\varphi) + k_c^2 \sin^2(\varphi)\right] + \frac{\rho' \left[1 + k_c^2 - (1-k_c^2)\rho'\right]}{z'^2 + (1+\rho')^2} \sin^2(\varphi) \right\} .
\end{aligned}
\tag{A.120}
$$

Consider for now only the part inside the {} of above equation:

$$
\begin{aligned}
&\left(1-\frac{\rho'(1+\rho')}{z'^2+(1+\rho')^2}\right)\left[\cos^2(\varphi)+k_c^2\sin^2(\varphi)\right]+\frac{\rho'\left[1+k_c^2-(1-k_c^2)\rho'\right]}{z'^2+(1+\rho')^2}\sin^2(\varphi)\\
&=\frac{1}{z'^2+(1+\rho')^2}\left\{\left[z'^2+(1+\rho')^2-\rho'(1+\rho')\right]\left[\cos^2(\varphi)+k_c^2\sin^2(\varphi)\right]\right.\\
&\qquad\left.+\rho'\left[1+k_c^2-(1-k_c^2)\rho'\right]\sin^2(\varphi)\right\} \qquad \text{(A.121)}
\end{aligned}
$$

and in there also only the part inside the {}:

$$
\begin{aligned}
&\left[z'^2+(1+\rho')^2-\rho'(1+\rho')\right]\left[\cos^2(\varphi)+k_c^2\sin^2(\varphi)\right]\\
&+\rho'\left[1+k_c^2-(1-k_c^2)\rho'\right]\sin^2(\varphi)\\
&=\left[z'^2+(1+\rho')^2-\rho'(1+\rho')\right]\left[\cos^2(\varphi)+\frac{z'^2+(1-\rho')^2}{z'^2+(1+\rho')^2}\sin^2(\varphi)\right]\\
&+\rho'\left[1+k_c^2-(1-k_c^2)\rho'\right]\sin^2(\varphi)\\
&=\left[z'^2+(1+\rho')^2\right]\cos^2(\varphi)+\left[z'^2+(1-\rho')^2\right]\sin^2(\varphi) \qquad \Big\}\equiv(*)\\
&-\rho'(1+\rho')\left[\cos^2(\varphi)+k_c^2\sin^2(\varphi)\right]+\rho'\left[1+k_c^2-(1-k_c^2)\rho'\right]\sin^2(\varphi)\,. \qquad \Big\}\equiv(**)
\end{aligned}
\qquad \text{(A.122)}
$$

The two contributions are simplified separately:

$$
\begin{aligned}
(*)=&\left[z'^2+1+2\rho'+\rho'^2\right]\cos^2(\varphi)+\left[z'^2+1-2\rho'+\rho'^2\right]\sin^2(\varphi)\\
=&\,z'^2+1+\rho'^2+2\rho'\left[\cos^2(\varphi)-\sin^2(\varphi)\right] \qquad \text{(A.123)}
\end{aligned}
$$

as well as:

$$
\begin{aligned}
(**)=&-\rho'\cos^2(\varphi)-\rho'^2\cos^2(\varphi)\cancel{-\rho'k_c^2\sin^2(\varphi)}\cancel{-\rho'^2k_c^2\sin^2(\varphi)}\\
&+\rho'\sin^2(\varphi)\cancel{+\rho'k_c^2\sin^2(\varphi)}-\rho'^2\sin^2(\varphi)\cancel{+\rho'^2k_c^2\sin^2(\varphi)}\\
=&-\rho'\left[\cos^2(\varphi)-\sin^2(\varphi)\right]-\rho'^2\underbrace{\left[\cos^2(\varphi)+\sin^2(\varphi)\right]}_{=1} \qquad \text{(A.124)}
\end{aligned}
$$

Combining them to form Eqn. (A.122) leads to:

$$
\begin{aligned}
(*)+(**)=&\,z'^2+1\cancel{+\rho'^2}+\cancel{2}\rho'\left[\cos^2(\varphi)-\sin^2(\varphi)\right]\cancel{-\rho'\left[\cos^2(\varphi)-\sin^2(\varphi)\right]}\cancel{-\rho'^2}\\
=&\,z'^2+1+\rho'\left[\cos^2(\varphi)-\sin^2(\varphi)\right]\,. \qquad \text{(A.125)}
\end{aligned}
$$

The full form of B_z is assembled again now based on the recent findings to remind ourselves of the state of things:

$$B_z = \frac{\mu_0 I}{\pi a} \frac{1}{\rho' \sqrt{z'^2 + (1+\rho')^2}}$$
$$\int\limits_0^{\pi/2} \frac{\sin^2(\varphi) - \cos^2(\varphi)}{\left[\cos^2(\varphi) + k_c^2 \sin^2(\varphi)\right]^{3/2}} \frac{1}{z'^2 + (1+\rho')^2} \left\{ z'^2 + 1 + \rho' \left[\cos^2(\varphi) - \sin^2(\varphi)\right] \right\} \mathrm{d}\varphi \, . \tag{A.126}$$

The term in {} in above integrand is now restructured :

$$\begin{aligned}
& z'^2 + 1 + \rho' \left[\cos^2(\varphi) - \sin^2(\varphi)\right] \\
= & \frac{1}{2} z'^2 + \frac{1}{2}\left(z'^2 + 1 - \rho'^2\right) + \frac{1}{2}\left\{1 + \rho'^2 + 2\rho' \left[\cos^2(\varphi) - \sin^2(\varphi)\right]\right\} \\
= & \quad \frac{1}{2} z'^2 \left[\cos^2(\varphi) + \sin^2(\varphi)\right] + \frac{1}{2}\left(z'^2 + 1 - \rho'^2\right) \\
& + \frac{1}{2}\Big[\underbrace{\left(1 + 2\rho' + \rho'^2\right)}_{=(1+\rho')^2} \cos^2(\varphi) + \underbrace{\left(1 - 2\rho' + \rho'^2\right)}_{=(1-\rho')^2} \sin^2(\varphi)\Big] \\
= & \frac{1}{2}\left[z'^2 + (1+\rho')^2\right] \cos^2(\varphi) + \frac{1}{2}\left[z'^2 + (1-\rho')^2\right] \sin^2(\varphi) + \underbrace{\frac{1}{2}\left(z'^2 + 1 + \rho'^2\right)}_{(*)} \underbrace{-\rho'^2}_{(**)} \, .
\end{aligned} \tag{A.127}$$

Consider $(*)$ and $(**)$ separately:

$$\begin{aligned}
(*) &= \frac{1}{2} z'^2 + \frac{1}{4}\Big[\underbrace{1 + 2\rho' + \rho'^2}_{=(1+\rho')^2} + \underbrace{1 - 2\rho' + \rho'^2}_{=(1-\rho')^2}\Big] \\
&= \frac{1}{4}\left[z'^2 + (1+\rho')^2 + z^2 + (1-\rho')^2\right] \\
&= \frac{1}{4}\left[z'^2 + (1+\rho')^2\right] + \frac{1}{4}\left[z^2 + (1-\rho')^2\right]
\end{aligned} \tag{A.128}$$

and

$$\begin{aligned}
(**) &= \frac{1}{4}\rho' \left[z'^2 + 1 - 2\rho' + \rho'^2 - \left(z'^2 + 1 + 2\rho' + \rho'^2\right)\right] \\
&= \frac{1}{4}\rho' \left[z'^2 + (1-\rho')^2\right] - \frac{1}{4}\rho' \left[z'^2 + (1+\rho')^2\right] \, .
\end{aligned} \tag{A.129}$$

These expressions are now inserted into Eqn. (A.127), leading to:

$$
\begin{aligned}
&\frac{1}{2}\left[z'^2+(1+\rho')^2\right]\cos^2(\varphi)+\frac{1}{2}\left[z'^2+(1-\rho')^2\right]\sin^2(\varphi)\\
&+\frac{1}{4}\left[z'^2+(1+\rho')^2\right]+\frac{1}{4}\left[z^2+(1-\rho')^2\right]\\
&+\frac{1}{4}\rho'\left[z'^2+(1-\rho')^2\right]-\frac{1}{4}\rho'\left[z'^2+(1+\rho')^2\right]\\
=&\left[z'^2+(1+\rho')^2\right]\left\{\frac{1}{2}\cos^2(\varphi)+\underbrace{\frac{z'^2+(1-\rho')^2}{z'^2+(1+\rho')^2}}_{=k_c^2}\sin^2(\varphi)\right.\\
&\qquad\left.+\frac{1}{4}\left[1+\underbrace{\frac{z'^2+(1-\rho')^2}{z'^2+(1+\rho')^2}}_{=k_c^2}-\left(1-\underbrace{\frac{z'^2+(1-\rho')^2}{z'^2+(1+\rho')^2}}_{=k_c^2}\right)\rho'\right]\right\}\\
=&\left[z'^2+(1+\rho')^2\right]\left\{\frac{1}{2}\left[\cos^2(\varphi)+k_c^2\sin^2(\varphi)\right]+\frac{1}{4}\left[1+k_c^2-\left(1-k_c^2\right)\rho'\right]\right\}.
\end{aligned}
\tag{A.130}
$$

This is now inserted back into Eqn. (A.126):

$$
\begin{aligned}
B_z=\frac{\mu_0 I}{\pi a}\frac{1}{\rho'\sqrt{z'^2+(1+\rho')^2}}\int\limits_0^{\pi/2}&\frac{\sin^2(\varphi)-\cos^2(\varphi)}{\left[\cos^2(\varphi)+k_c^2\sin^2(\varphi)\right]^{3/2}}\\
&\left\{\frac{1}{2}\left[\cos^2(\varphi)+k_c^2\sin^2(\varphi)\right]+\frac{1}{4}\left[1+k_c^2-\left(1-k_c^2\right)\rho'\right]\right\}\mathrm{d}\varphi\,.
\end{aligned}
\tag{A.131}
$$

The integral can be split up back again into two integrals:

$$
\begin{aligned}
B_z=\frac{\mu_0 I}{\pi a}\frac{1}{\rho'\sqrt{z'^2+(1+\rho')^2}}&\left[\frac{1}{2}\underbrace{\int\limits_0^{\pi/2}\frac{\sin^2(\varphi)-\cos^2(\varphi)}{\sqrt{\cos^2(\varphi)+k_c^2\sin^2(\varphi)}}\,\mathrm{d}\varphi}_{=\mathrm{cel}(k_c,1,-1,1)}\right.\\
&\left.+\frac{1}{4}\left[1+k_c^2-\left(1-k_c^2\right)\rho'\right]\underbrace{\int\limits_0^{\pi/2}\frac{\sin^2(\varphi)-\cos^2(\varphi)}{\left[\cos^2(\varphi)+k_c^2\sin^2(\varphi)\right]^{3/2}}\,\mathrm{d}\varphi}_{=\mathrm{cel}(k_c,k_c^2,-1,1)}\right].
\end{aligned}
\tag{A.132}
$$

This concludes the derivation of the expression for B_z of a circular wire loop and here is the final result as published in Ref. [8]:

$$\boxed{B_z(\rho', z') = \frac{\mu_0 I}{2\pi a} \frac{1}{\rho' \sqrt{z'^2 + (1+\rho')^2}} \left[\mathrm{cel}(k_c, 1, -1, 1) + \frac{1 + k_c^2 - (1 - k_c^2)\,\rho'}{2} \mathrm{cel}(k_c, k_c^2, -1, 1) \right]} \tag{A.133}$$

Appendix B. Derivation of Special Case Formulations

Appendix C. Reference Data

Reference outputs have been computed using the `mpmath` Python package [2]. The reference implementation was tested at a subset of the test points against Mathematica [3]. The results are listed in Table C.1.

case	ρ'	z'	A_φ / Tm
0	0	0	`0.0000000000000000e+00`
1	10^{-15}	0	`3.5499996985564660e-20`
2	0.5	0	`1.9733248350774467e-05`
3	2	0	`9.8666241753872340e-06`
4	10^{15}	0	`3.5499996985564664e-35`
5	0	10^{-15}	`0.0000000000000000e+00`
6	10^{-15}	10^{-15}	`3.5499996985564660e-20`
7	0.5	10^{-15}	`1.9733248350774467e-05`
8	2	10^{-15}	`9.8666241753872340e-06`
9	10^{15}	10^{-15}	`3.5499996985564664e-35`
10	0	1	`0.0000000000000000e+00`
11	10^{-15}	1	`1.2551144300297384e-20`
12	0.5	1	`5.8203906810256120e-06`
13	1	1	`8.8857583532073070e-06`
14	2	1	`6.2831799875378960e-06`
15	10^{15}	1	`3.5499996985564664e-35`
16	0	10^{15}	`0.0000000000000000e+00`
17	10^{-15}	10^{15}	`3.5499996985564664e-65`
18	0.5	10^{15}	`1.7749998492782333e-50`
19	1	10^{15}	`3.5499996985564666e-50`
20	2	10^{15}	`7.0999993971129330e-50`
21	10^{15}	10^{15}	`1.2551144300297385e-35`

Table C.1: Reference outputs for testing an implementation of Eqn. (A.95), computed using arbitrary-precision arithmetic. The displayed values for A_φ are rounded to the nearest 64-bit `double` precision value (IEEE 754). The loop current was chosen as $I = 113\,\mathrm{A}$.

References

[1] J. D. Hanson, S. P. Hirshman, Compact expressions for the Biot-Savart fields of a filamentary segment, Physics of Plasmas 9 (2012) 4410–4412. doi:10.1063/1.1507589.

[2] F. Johansson, et al., mpmath: a Python library for arbitrary-precision floating-point arithmetic (version 0.18), http://mpmath.org/ (December 2013).

[3] Wolfram Research, Inc., Mathematica, Version 12.1, Champaign, IL, 2021.
URL https://www.wolfram.com/mathematica

[4] P. L. Walstrom, Algorithms for Computing the Magnetic Field, Vector Potential, and Field Derivatives for Circular Current Loops in Cylindrical Coordinates (2017) LA–UR–17–27619doi:10.2172/1377379.

[5] J. D. Jackson, Classical Electrodynamics, 5th Edition, Wiley, New York, NY, 2014.

[6] I. N. Bronstein, K. A. Semendjajew, Taschenbuch der Mathematik, 19th Edition, BSB B. G. Teubner Verlagsgesellschaft, Nauka-Verlag, Leipzig, Moskau, 1979.

[7] R. Bulirsch, Numerical Calculation of Elliptic Integrals and Elliptic Functions. III 13 (1969) 305 – 315. doi:10.1007/BF02165405.

[8] J. Belcher, S. Olbert, N. Derby, TEAL Physics and Mathematics Documentation, accessed 2021-09-02 (2008).
URL http://web.mit.edu/viz/soft/visualizations/tealsim/downloads/TEAL_Physics_Math.pdf